ChemComm

COMMUNICATION

View Article Online
View Journal | View Issue

Cite this: *Chem. Commun.*, 2019, **55**, 12663

Received 2nd September 2019,
Accepted 23rd September 2019

DOI: 10.1039/c9cc06829e

rsc.li/chemcomm

Cation–π interactions secure aggregation induced emission of planar organic luminophores†

Kaspars Leduskrasts, Artis Kinens and Edgars Suna *

The use of non-covalent intermolecular π^+–π interactions between quaternary pyridinium or imidazolium cations and aromatic π systems is an efficient approach to achieve AIE in planar purely organic luminophores.

Organic luminophores that are highly emissive in dilute solutions frequently experience decrease or even loss of the emission upon aggregation. This phenomenon is known as aggregation-caused quenching (ACQ).[1] The ACQ is a major hurdle in many practical applications, which require emission in the aggregated state (thin films, polymer matrices, *etc.*) or in the solid state.[2–6] In 2001 Tang discovered aggregation induced emission luminogens (AIEgens) that featured increased emission in the solid state as compared to that in dilute solution.[7] Since then AIEgens have found ample applications in various optoelectronic devices such as OLEDs,[8] organic field-effect transistors[5,9] and photovoltaic devices[10] as well as in artificial photosynthesis[11] and photon refining.[12] AIEgens have also been widely used as chemical sensors,[13] biosensors,[14] stimuli sensors[15] and as luminescent probes in biomedical applications.[16]

The working principle underlying the emission of AIEgens is proposed to be a restriction of intramolecular motions (RIM), vibrations (RIV) and rotations (RIR) to minimize the non-radiative dissipation of exciton energy.[16b,17] In addition, the design of AIEgens also frequently features out-of-plane twisting of aromatic subunits and incorporation of a steric bulk to avoid the detrimental intermolecular π–π stacking interactions between planar aromatic luminophores, which results in the ACQ effect. These structural requirements usually lead to a relatively complex design of purely organic AIEgens.[16a,b,18] Clearly, a new type of interaction that would help to achieve AIE in structurally simple purely organic molecules is highly desired for the development of AIEgens.

Recently we have demonstrated that non-covalent intermolecular interactions between pyridinium (Py^+) cations (π^+–π^+ interactions) leads to a solid state luminescence (SSL) with up to 19% PLQY (see Fig. 1).[19] In this study we report on a further development of the conceptual approach to achieve AIE. Specifically, we show herein that a mechanistically related interaction between quaternary Py^+ or imidazolium (Im^+) cations and aromatic π systems (π^+–π interactions) results in remarkable SSL (up to 80% PLQY). Furthermore, the quaternization of nitrogen atoms turns on the SSL even in planar heteroaromatic molecules (Fig. 1). The performed DFT calculations suggest that the observed SSL results from intermolecular charge transfer (ICT) between heteroaromatic (Py^+ and Im^+) cations and aromatic π systems.

Py^+ and Im^+ perchlorates **3a–d** were obtained by *N*-alkylation of the commercially available heterocycles **1a–d** with MeI, followed by the exchange of iodide for perchlorate (Fig. 2). Pyridines **5a,b** were synthesized from the commercially available **4** and pyridine boronic acids under Suzuki reaction conditions. Subsequent *N*-alkylation with MeI was followed by iodide-to-perchlorate exchange to afford Py^+ salts **7a,b**. The synthesis of heterocycles **5c** and **5d** required Cu(I)-catalyzed *N*-arylation of carbazole by the commercially available bromides **8** and **9**, respectively. A subsequent *N*-alkylation and anion exchange sequence provided **7c,d** (Fig. 2). All heteroaromatic quaternary salts **3a–d**, **6a** and **7a–d** were crystalline materials.

UV-vis spectra of all synthesized quaternary salts and parent heterocycles were measured in MeCN solutions (at *ca.* 10^{-5} mol L^{-1}) at room temperature and under an ambient atmosphere.

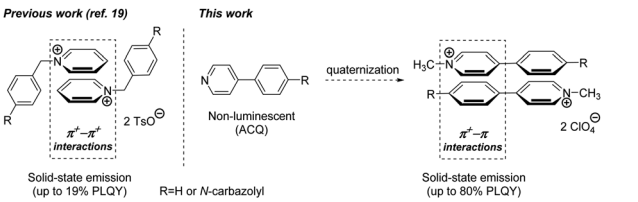

Fig. 1 Design of the solid state AIEgens by intermolecular cation–π interactions.

Latvian Institute of Organic Synthesis, Aizkraukles 21, Riga, LV-1006, Latvia. E-mail: edgars@osi.lv

† Electronic supplementary information (ESI) available: Experimental procedures, photo physical properties, X-ray crystallographic data (CIF files), DFT calculations, and ^{1}H and ^{13}C NMR spectra. CCDC 1949701–1949703. For ESI and crystallographic data in CIF or other electronic format see DOI: 10.1039/c9cc06829e

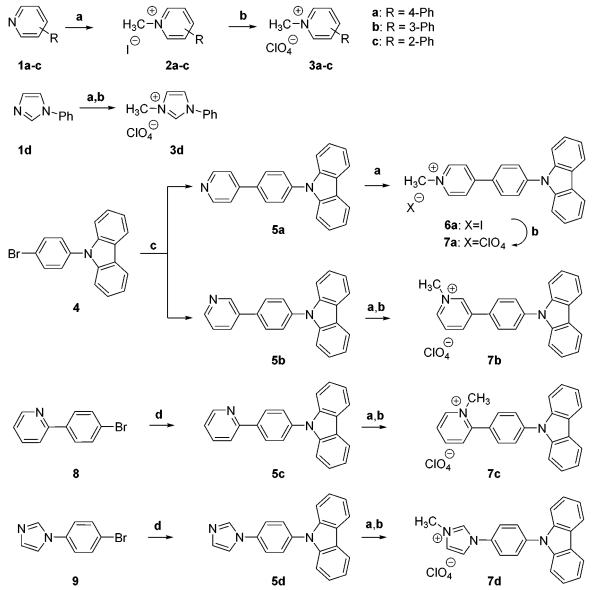

Fig. 2 Synthesis of heteroaromatic salts **2a**, **3a–d**, **6a** and **7a–d**. *Reagents and conditions*: (a) CH_3I, MeCN, 80 °C, 16 h, 96% (**2a**), 94% (**6a**). (b) $AgClO_4$, MeCN, r.t., 15 min, 70% (**3a**), 61% (**3b**), 88% (**3c**), 64% (**3d**), 98% (**7a**), 94% (**7b**), 54% (**7c**), 94% (**7d**). (c) Pyridine-4-boronic acid (for **5a**) or pyridine-3-boronic acid (for **5b**), $Pd(dppf)Cl_2$ × DCM (5 mol%), K_2CO_3, 1 : 6 water–MeCN, 90 °C, 1 h, 75% (**5a**), 72% (**5b**). (d) Carbazole, CuI (15 mol%), L-Pro (30 mol%), K_2CO_3, DMSO, 120–140 °C, 16–72 h, 22% (**5c**), 47% (**5d**).

For analysis of absorption spectra, see Table 1 and the ESI,† page S16. Heteroarenes **1a–d** did not show any measurable emission in solution and in the solid state with <0.1% photoluminescence quantum yields (PLQYs). The lack of emission for **1a–d** was not surprising because these molecules do not possess any of the traditional luminophore moieties such as carbazole. Alkylation of **1a** with MeI afforded Py^+ iodide **2a**, which displayed a broad non-structured emission band at λ_{max} = 372 nm in MeCN solution with 36.8% PLQY (entry 1, Table 1).[20] Unfortunately, Py^+ salt **2a** was non-emissive in the solid state, and the lack of SSL for Py^+ iodides has been reported earlier by Fossey.[21] We were pleased to find that a simple exchange of iodide **2a** to perchlorate **3a** enabled high SSL (λ_{max} = 346 nm, 52.7% PLQY), while retaining the emission in MeCN solution (broad emission band at λ_{max} = 372 nm with 37.9% PLQY; entry 2). Isomeric perchlorates **3b,c** also displayed observable emission in solution (at λ_{max} = 390 nm and 380 nm with PLQYs of 21.1% and 3.5%, respectively) and high SSL with PLQYs of 42.1% (λ_{max} = 350 nm) and 39.1% (λ_{max} = 341 nm), respectively (entries 3 and 4). Decreased PLQY for **3c** both in solution and in the solid state could be possibly attributed to the decreased conjugation due to the presence of a *N*-methyl substituent. We were also pleased to find that SSL can be achieved using cationic heteroaromatic subunits other than Py^+ salts. Thus, Im^+ perchlorate **3d** showed luminescence both in solution (λ_{max} = 380 nm, 16.1% PLQY) and in the solid state (λ_{max} = 315 nm, 19.8% PLQY; entry 5). Notably, all perchlorates **3a–d** featured AIE properties as evidenced by higher PLQY in the solid state as compared to solution (α_{AIE} up to 11.2; see Table 1). The observed SSL levels for **3a–d** (up to 53% PLQY for **3a**) are remarkable given the structural simplicity of salts **3a–d** and the absence of a luminophore moiety in their structure.

Next, we incorporated carbazole into AIEgens **3a–d** to increase their luminescence efficiency. Highly intense SSL was observed for perchlorates **7a** (79.8% PLQY at λ_{max} = 489 nm), **7b** (72.2% PLQY at λ_{max} = 446 nm) and **7c** (46.9% PLQY at λ_{max} = 465 nm; entries 11–13). Strikingly, Py^+ perchlorates **7a–c** were non-emissive in MeCN solution with PLQY < 0.1%. The observed up to 800-fold increase of PLQY in the solid state as compared to that in the MeCN solution confirms the AIE nature of **7a–c**. Perchlorate **7d** demonstrated slightly reduced SSL (11.0% PLQY at λ_{max} = 498 nm; entry 14) *vs.* parent **3d** (entry 5). In contrast to perchlorate **7a**, the corresponding iodide **6a** showed luminescence neither in the MeCN solution nor in the solid state (entry 10). The observed lack of the luminescence for iodides **2a** and **6a** demonstrates the importance of the counter-ion in the quaternized luminophores. Finally, the luminescence properties of parent **5a–d** were also determined. All non-charged heterocycles **5a–d** featured high emission intensity in MeCN solutions (entries 6–9) with **5a** showing the highest PLQY (73.1%). In contrast, considerably reduced SSL was observed for **5a–d**. Thus, **5b** showed up to 80-fold decrease of PLQY in the solid state as compared to the MeCN solution (entry 7). Evidently, the reduced SSL is a result of the ACQ effect in the highly planar luminophores **5a–d**, which experience intermolecular π–π aromatic interactions leading to decay of the

Table 1 Photoluminescence properties of luminophores **2a–7d**

Entry	Compound	λ_{abs}, nm	Solution λ_{em}, nm	Solid λ_{em}, nm	Solution, ϕ (%)	Solid, ϕ (%)	α_{AIE}
1	**2a**	247, 293	372	—	36.8	<0.1	<0.1
2	**3a**	231, 294	372	346	37.9	52.7	1.4
3	**3b**	237, 257, 292	390	350	21.2	42.1	2.0
4	**3c**	239, 282	380	341	3.5	39.1	11.2
5	**3d**	235	353	315	16.1	19.8	1.2
6	**5a**	238, 292, 322	442	371, 387, 407	73.1	5.7	0.1
7	**5b**	240, 292, 338	408	368	46.5	0.6	<0.1
8	**5c**	240, 292, 315	416	378, 436	74.6	16.8	0.2
9	**5d**	240, 292, 326, 339	347, 361	371	33.2	17.8	0.5
10	**6a**	237, 282, 376	—	473	<0.1	0.40	>4
11	**7a**	239, 282, 379	—	489	<0.1	79.8	>800
12	**7b**	236, 289, 339	—	446	<0.1	72.2	>700
13	**7c**	237, 279, 337	—	465	<0.1	46.9	>470
14	**7d**	241, 291, 336	498	369	1.6	11.0	6.9

excited-state energy *via* non-radiative energy transfer.[22] In contrast, ACQ does not affect the structurally related planar salts **7a–d** as evidenced by the pronounced AIE properties of these luminophores. Furthermore, the change in structured emission for **5a** in the solid state to a broad featureless solid state emission of perchlorate **7a** indicates distinct emission mechanisms for **5a** and **7a**.

The AIE properties of perchlorates **7a–d** were further corroborated by the observed correlation between the emission and formation of aggregates (see the ESI,† page S27, for details). In addition, lack of emission for **7a** in solution and the frozen DMSO matrix (solid amorphous state) speaks against the RIR effect as the origin of the AIE properties of quaternary salts **3a–d** and **7a–d** (see the ESI,† page S29, for details). A notable feature of perchlorates **3a–d** and **7d** is the SSL in the UV region (315–369 nm; entries 2–5 and 14), a property that has been rarely observed for AIE materials.[23] The attachment of the carbazole moiety to **3a–d** resulted in a substantial (54–143 nm) red-shift of the SSL. Hence, the introduction of electron donating moieties in **3a–d** shifts the emission maxima, allowing for direct control of the emission wavelength.

Single crystal X-ray analysis of **3a**, **6a** and **7a** provided important insight into the intermolecular interactions that lead to the SSL (Table 2). In a crystal lattice, salts **3a**, **6a** and **7a** showed close interactions between charged Py^+ cations and π systems (π^+–π interactions), which ranged from 3.500 Å (**6a**) to 3.760 Å (**3a**; Table 2). However, the distance between centroids does not correlate with the emission efficiency. Thus, very low PLQY (0.4%) was observed for **6a** in the solid state despite the short distances for π^+–π interactions (3.500 Å and 3.652 Å). Salt **7a** also featured short distance between Py^+ cations and carbazole π-systems (3.525 Å), whereas the corresponding distance in **3a** was longer (3.760 Å). Nevertheless, both **3a** and **7a** were superior to **6a** with respect to the SSL efficiency (52.7% and 79.8% PLQY, respectively). The interacting Py^+ and carbazole planar rings are nearly parallel in **6a** and **7a** (5.65° and 3.73° angles between the planes of heterocycles, respectively), and the angle between the Py^+ subunit and arene ring in **3a** is 19.1°. Despite the apparent similarity between the packing mode of **6a** and **7a**, the remarkable difference in the solid state PLQY suggests that the iodide ion quenches the emission in **6a** by mechanisms other than steric or electronic hindrance of the π^+–π interactions.

Additional support for the relationship between π^+–π interactions (involving Py^+ cations and carbazole π systems) and the SSL was obtained by time-dependent density functional theory (TDDFT) calculations of the emission spectra for **7a** at the B3LYP/6-31G(d) level of theory (see the ESI,† page S33). As Py^+ perchlorate **7a** did not display emission in solution, the emission spectra of **7a** were calculated using geometry from the crystalline state. Furthermore, only singlet states S_n were used for calculations because oxygen quenching experiments in the suspensions of **7a** did not show any emission intensity change, thus providing evidence against triplet state emission.

First, the feasibility of intramolecular CT character of the SSL in cation **7a** was examined at the single molecule level. The calculated emission spectra (Fig. 3A) displayed two distinct emission peaks at λ_{max} = 341 nm and 740 nm with high oscillatory force (f = 0.3387 and f = 0.3063; see Fig. 3A). Molecular orbitals (MO) associated with the electronic transitions were localized in the carbazole moiety (HOMO) and in the Py^+ moiety with lesser intensity occupying also the phenylene linker (LUMO; see Fig. 3C and the ESI,† page S33, for the representation of frontier MO). The emission peak at λ_{max} = 341 nm corresponded to transition from HOMO−4 to the LUMO and from the HOMO to LUMO+3. The emission peak at λ_{max} = 740 nm corresponded to transition from the HOMO to LUMO (see Fig. 3B and the ESI†). Notably, the calculated emission peaks did not match the experimentally observed one at λ_{max} = 489 nm (Table 1, entry 11). Consequently, an intramolecular CT apparently does not account for the observed SSL of **7a**.

Next, the emission spectra for the symmetric dimer of **7a** were calculated, resulting in a broad emission peak at λ_{max} = 495 nm with a large oscillatory force (f = 0.3784; Fig. 3C). MO associated with the electronic transitions was localized in two regions of the dimer: the HOMO was located on the carbazole moiety, whereas the LUMO was mostly localized on the Py^+ moiety with lesser intensity occupying also the phenylene linker (see Fig. 3C and the ESI† for the representation of the frontier MO). Calculations show that multiple CT (from HOMO−3 to the LUMO, from HOMO−2 to LUMO+1, from HOMO−1 to LUMO and from HOMO to LUMO+1; see the ESI†) are responsible for the emission at λ_{max} = 495 nm. Such a type of symmetric

Table 2 Crystal packing of salts **3a**, **6a** and **7a**

3a	**6a**	**7a**
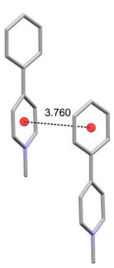	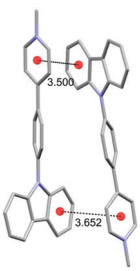	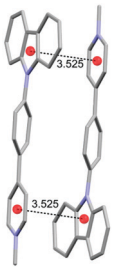

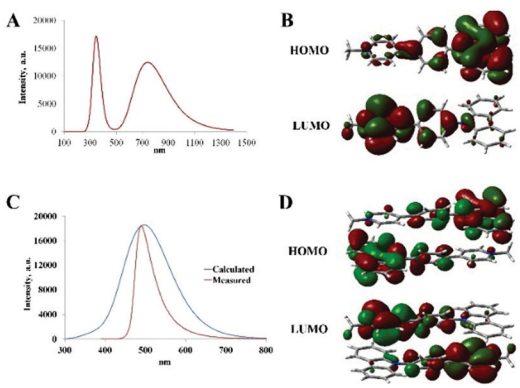

Fig. 3 (A) Calculated UV-Vis spectrum of **7a** (single molecule). (B) Frontier MO for **7a** (single molecule). (C) Calculated UV-Vis spectrum of the dimer of **7a**. (D) Frontier MO for the dimer of **7a**.

through-space CT has been reported for the SSL.[24] Notably, the calculated emission at λ_{max} = 495 nm for the dimer of **7a** was consistent with that observed experimentally (λ_{max} = 489 nm; entry 11). However, the observed SSL peak for **7a** was narrower compared to the calculated one. This difference could be possibly attributed to the additional stabilizing interactions in the crystal lattice for **7a**. Consequently, the TDDFT calculations provide evidence that an emissive intermolecular through-space CT band is responsible for the SSL of cationic perchlorates **3a–d** and **7a–d**.

In summary, a series of highly emissive planar AIEgens has been designed by utilizing non-covalent intermolecular π^+–π interactions between Py^+ or Im^+ cations and aromatic π systems. Structurally simple salts **3a–d** lacking any conventional luminophore moiety demonstrated high SSL (up to 53% PLQY) in the UV region (315–350 nm). The introduction of electron donating moieties in **3a–d** resulted in bathochromic shifts of the emission maxima, thus allowing for direct control of emission wavelength. Carbazole-containing perchlorates **7a–d** also demonstrated a remarkable (up to 800-fold) increase of PLQY as compared to that in MeCN solution. The presence of iodide ions led to the quenching of the SSL. Single crystal X-ray analyses confirm the presence of non-covalent intermolecular interactions between Py^+ or Im^+ cations and aromatic π systems in the crystal state of AIEgens **3a** and **7a**. TDDFT calculations provide strong evidence that the observed SSL of **3a–d** and **7a–d** is a result of intermolecular π^+–π interactions that generate through-space CT bands in the crystal state. The use of the non-covalent π^+–π interactions in the design of AIEgens is a complementary approach to routinely used means to achieve AIE properties and to avoid the ACQ effect. We believe that our study will expand the scope of structural motifs that previously could not be used due to the ACQ and will open a new avenue for the rational design of AIEgens.

This work was funded by ERDF project No. 1.1.1.1/18/A/063. We thank Dr S. Belyakov and Dr A. Mishnev for X-ray crystallographic analysis and P. Dimitrijevs for DLS measurements.

Conflicts of interest

There are no conflicts to declare.

Notes and references

1 (*a*) A. S. Klymchenko, *Acc. Chem. Res.*, 2017, **50**, 366; (*b*) S. A. Jenekhe and J. A. Osaheni, *Science*, 1994, **265**, 765.
2 R. B. Thompson, *Fluorescence Sensors and Biosensors*, CRC/Taylor & Francis, Boca Raton, 2006.
3 C. D. Geddes and J. R. Lakopwicz, *Advanced Concepts in Fluorescence Sensing*, Springer, New York, 2005.
4 A. Buckley, *Organic light-emitting diodes (OLEDs): materials, devices and applications*, Woodhead Publishing, Oxford, 2013.
5 S. G. Surya, H. N. Raval, R. Ahmad, P. Sonar, K. N. Salama and V. R. Rao, *TrAC, Trends Anal. Chem.*, 2019, **111**, 27.
6 E. Fresta and R. D. Costa, *J. Mater. Chem. C*, 2017, **5**, 5643.
7 J. Luo, Z. Xie, J. W. Y. Lam, L. Cheng, H. Chen, C. Qiu, H. S. Kwok, X. Zhan, Y. Liu, D. Zhu and B. Z. Tang, *Chem. Commun.*, 2001, 1740.
8 (*a*) Z. Ning, Z. Chen, Q. Zhang, Y. Yan, S. Qian, Y. Cao and H. Tian, *Adv. Funct. Mater.*, 2007, **17**, 3799; (*b*) J. Huang, N. Sun, Y. Dong, R. Tang, P. Lu, P. Cai, Q. Li, D. Ma, J. Qin and Z. Li, *Adv. Funct. Mater.*, 2013, **23**, 2329.
9 (*a*) Z. Zhao, Z. Li, J. W. Y. Lam, J.-L. Maldonado, G. Ramos-Ortiz, Y. Liu, W. Yuan, J. Xu, Q. Miao and B. Z. Tang, *Chem. Commun.*, 2011, **47**, 6924; (*b*) M. P. Aldred, G.-F. Zhang, C. Li, G. Chen, T. Chen and M.-Q. Zhu, *J. Mater. Chem. C*, 2013, **1**, 6709.
10 (*a*) B. Mi, Y. Dong, Z. Li, J. W. Y. Lam, M. Haussler, H. H. Sung, H. S. Kwok, Y. Dong, I. D. Williams, Y. Liu, Y. Luo, Z. Shuai, D. Zhu and B. Z. Tang, *Chem. Commun.*, 2005, 3583; (*b*) Y. Li, Z. Li, Y. Wang, A. Compaan, T. Ren and W.-J. Dong, *Energy Environ. Sci.*, 2013, **6**, 2907.
11 (*a*) M. Zhang, X. Yin, T. Tian, Y. Liang, W. Li, Y. Lan, J. Li, M. Zhou, Y. Ju and G. Li, *Chem. Commun.*, 2015, **51**, 10210; (*b*) Y. Zeng, P. Li, X. Liu, T. Yu, J. Chen, G. Yang and Y. Li, *Polym. Chem.*, 2014, **5**, 5978.
12 (*a*) P. Duan, D. Asthana, T. Nakashima, T. Kawai, N. Yanai and N. Kimizuka, *Faraday Discuss.*, 2017, **196**, 305; (*b*) L. Li, Y. Zeng, T. Yu, J. Chen, G. Yang and Y. Li, *ChemSusChem*, 2017, **10**, 4610.
13 (*a*) X. Wang, J. Hu, T. Liu, G. Zhang and S. Liu, *J. Mater. Chem.*, 2012, **22**, 8622–8628; (*b*) Y. Chen, W. Zhang, Y. Cai, R. T. K. Kwok, Y. Hu, J. W. Y. Lam, X. Gu, Z. He, Z. Zhao, X. Zheng, B. Chen, C. Gui and B. Z. Tang, *Chem. Sci.*, 2017, **8**, 2047.
14 X. Xue, Y. Zhao, L. Dai, X. Zhang, X. Hao, C. Zhang, S. Huo, J. Liu, C. Liu, A. Kumar, W. Q. Chen, G. Zou and X. J. Liang, *Adv. Mater.*, 2014, **26**, 712.
15 (*a*) J. Q. Shi, W. J. Zhao, C. H. Li, Z. P. Liu, Z. S. Bo, Y. P. Dong, Y. Q. Dong and B. Z. Tang, *Chin. Sci. Bull.*, 2013, **58**, 2723; (*b*) Q. Qi, X. Fang, Y. Liu, P. Zhou, Y. Zhang, B. Yang, W. Tian and S. X.-A. Zhang, *RSC Adv.*, 2013, **3**, 16986.
16 (*a*) Y. Tang and B. Z. Tang, *Principles and Applications of Aggregation-Induced Emission*, Springer International Publishing, New York, 2019; (*b*) J. Mei, N. L. C. Leung, R. T. K. Kwok, J. W. Y. Lam and B. Z. Tang, *Chem. Rev.*, 2015, **115**, 11718.
17 (*a*) C. Yuan, S. Saito, C. Camacho, T. Kowalczyk, S. Irle and S. Yamaguchi, *Chem. – Eur. J.*, 2014, **20**, 2193; (*b*) L. Yao, S. Zhang, R. Wang, W. Li, F. Shen, B. Yang and Y. Ma, *Angew. Chem., Int. Ed.*, 2014, **53**, 2119; (*c*) J. Liu, X. Zhang, X. Lu, P. He, L. Jiang, H. Dong and W. Hu, *Chem. Commun.*, 2013, **49**, 1199.
18 (*a*) X. Wang, S. Wang, J. Lv, S. Shao, L. Wang, X. Jing and F. Wang, *Chem. Sci.*, 2019, **10**, 2915; (*b*) S.-K. Kim, S.-Y. Oh and J.-W. Park, *Thin Solid Films*, 2008, **517**, 1349.
19 K. Leduskrasts and E. Suna, *RSC Adv.*, 2019, **9**, 460.
20 W. Chen, S. A. Elfeky, Y. Nonne, L. Male, K. Ahmed, C. Amiable, P. Axe, S. Yamada, T. D. James, S. D. Bull and J. S. Fossey, *Chem. Commun.*, 2011, **47**, 253.
21 I. Richter, M. R. Warren, J. Minari, S. A. Elfeky, W. Chen, M. F. Mahon, P. R. Raithby, T. D. James, K. Sakurai, S. J. Teat, S. D. Bull and J. S. Fossey, *Chem. – Asian J.*, 2009, **4**, 194.
22 See the ESI,† page S23, for further discussions.
23 (*a*) C.-Q. Ye, L.-W. Zhou, C.-B. Fan, G.-L. Dai, X.-M. Wang, X.-T. Tao, P.-Y. Tang and W.-M. Su, *ChemistrySelect*, 2019, **4**, 2044; (*b*) Z. Gan, M. Meng, Y. Di and S. Huang, *New J. Chem.*, 2016, **40**, 1970.
24 X.-H. Jin, C. Chen, C.-X. Ren, L.-X. Cai and J. Zhang, *Chem. Commun.*, 2014, **50**, 15878.

